Summer 2020

Intrinsic mechanical properties of zirconium carbide ceramics

Nicole Mary Korklan

Department:

INTRINSIC MECHANICAL PROPERTIES OF ZIRCONIUM CARBIDE CERAMICS

by

NICOLE MARY KORKLAN

A THESIS

Presented to the Faculty of the Graduate School of the

MISSOURI UNIVERSITY OF SCIENCE AND TECHNOLOGY

In Partial Fulfillment of the Requirements for the Degree

MASTERS OF SCIENCE IN CERAMIC ENGINEERING

2020

Approved by:

Gregory E. Hilmas, Advisor
William G. Fahrenholtz
Jeremy L. Watts

PUBLICATION THESIS OPTION

This thesis consists of the following manuscripts which have been or will be submitted for publication as follows.

Paper I: Pages 17-30 entitled "Processing and Room Temperature Properties of Zirconium Carbide" has been submitted to the Journal of the American Ceramic Society and is in review.

Paper II: Pages 31-43 entitled "Ultra High Temperature Strength of Zirconium Carbide" is being drafted for publication.

ABSTRACT

This research focuses on the processing and mechanical properties of zirconium carbide ceramics (ZrC_x). The first goal of this project was to densify near stoichiometric (i.e., x as close to 1 as possible) and nominally phase pure ZrC_x. The maximum stoichiometry achieved for the ZrC_x (C/Zr ratio of 0.92) was measured using gas fusion analysis. Hot pressing was used to obtain dense ZrC_x. Archimedes was used to determine the relative density of hot pressed ZrC_x at >95%. Scanning electron microscopy (SEM) was used to determine the overall microstructure of the hot pressed ZrC_x. The measured porosity was ~4 vol% and additional unreacted carbon was observed in SEM images. The average grain size was 2.7 ± 1.4 μm with a maximum observed grain size of 17.5 μm. The second goal of the project was to measure the hardness, flexure strength, and fracture toughness of ZrC_x at room temperature. Flexure strength at elevated temperatures, from 1600 to 2400°C, was also measured. Vickers' hardness was measured at two different loads and decreased from 19.5 GPa at a load of 0.5 kgf to 17.0 GPa at a load of 1 kgf. Flexure strength was 362.3 ± 46 MPa at room temperature and was roughly constant up to 2200°C where the strength decreased to 283 ± 34 MPa. Fracture toughness was determined to be 2.9 ± 0.1 $MPa \cdot m^{1/2}$ at room temperature. A Griffith-type analysis was used in determining the strength limiting flaws in the room temperature tests which was determined to be the largest grains of ZrC in the microstructure. The test bars used in the high temperature tests showed a slight increase in the average grain size but still within the standard deviation of the room temperature test bars.

ACKNOWLEDGEMENTS

First, I would like to thank my advisor, Dr. Gregory Hilmas, for his guidance and patience throughout my graduate studies and research. Next, I would like to thank Dr. William Fahrenholtz for providing advice and direction in my research. I would also like to thank Dr. Jeremy Watts for his assistance in the laboratory. I would like to thank NSF for providing the funding for this research with grant number DMR-1742086.

I would like to thank my peers in 307 for all there help and support. At the start of my graduate research they taught me how to operate the equipment needed for my research. They provided advice and kept me on track when I needed it most.

Finally, I would like to thank my family for their unending support and always believing in me. Without your support I would not have made it to where I am today. Thank you.

TABLE OF CONTENTS

LIST OF ILLUSTRATIONS

LIST OF TABLES

1. INTRODUCTION

Zirconium carbide (ZrC_x) has been researched for high-speed tooling, hypersonic vehicles, rocket nozzles, and nuclear reactor core materials.[1–6] ZrC_x is classified as an ultra-high temperature ceramic (UHTC) as it exhibits a melting temperature above 3000 °C. Most recently, ZrC_x is being considered for use in nuclear fuel applications. ZrC_x is attractive for use in nuclear reactors due to improved high temperature properties and resistance to nuclear fission product corrosion, as compared to SiC.[7] ZrC could therefore be a replacement for SiC as a structural and fission product barrier coating in Tri-structural Isotropic (TRISO) fuel particles, and as an oxygen getter in nuclear fuels.[2,5] ZrC_x has long been stated as a potential replacement for SiC in nuclear fuels due to its high melting point. While ZrC_x has favorable material properties that makes it attractive as a substitute for SiC, there are still some issues that require additional research. One reason that ZrC_x has not been made a replacement for SiC is due to the range of compositions that ZrC_x is stable in. ZrC_x exists over a wide range of carbon stoichiometries with a C/Zr ratio of 0.6-0.98. Impurities, such as hafnium, can also affect the properties of Zr based ceramics, as has been observed in ZrB_2 based ceramics.[8] Further, hafnium is a strong neutron absorber, so the impurity content in Zr-based ceramics would need to be controlled.[9]

Much of the current research on ZrC ceramics does not include the measured impurity content, or the carbon stoichiometry of the tested ZrC_x. The ZrC_x lattice can be stable with almost half of the carbon sites being vacancies. The wide stoichiometric range would surely have an effect on properties. Carbon vacancies affect the lattice parameter as well as the densification of ZrC. Further, oxygen and nitrogen can substitute for carbon

sites on the lattice, allowing for greater oxygen impurities in substoichiometric compositions of ZrC_x.

Understanding the impurities and carbon content in ZrC is important to be able to identify intrinsic properties. Some basic mechanical properties of ZrC_x have been reported in the technical literature.[9–11] The values reported in the literature vary widely, most likely due to the different ZrC_x stoichiometries, with the exact composition not always reported. The purpose of this research was to investigate the mechanical properties of near stoichiometric ZrC_x with low impurities, including low Hf, measured carbon stoichiometry, and known oxygen content.

2. LITERATURE REVIEW

The study of ZrC began during the 1950s and 1960s, when it was being researched for thermionic emissions to turn heat into energy.[14] In the 1970s and 1980s ZrC started to be researched as a potential replacement for silicon carbide (SiC), which is currently being used as a barrier coating material for TRISO (tri-isotropic) nuclear fuel.[5] More recently, this possibility has been re-investigated due to higher purity synthesis routes for ZrC becoming available. ZrC processed in these early studies contained various impurities, including hafnium, oxygen, nitrogen, and carbon. In a study by Leipold et al., the impurities of both hafnium and oxygen/nitrogen were measured to be as high as 2 wt%.[15] Another reason that ZrC was being studied was as a potential additive to uranium carbide (UC), designed to decrease the evaporation of uranium from the cathode of thermionic converters.[16] High temperature reactors (HTRs) are operated at temperatures in excess of 1600 °C, which is considered the upper limit for the current SiC technology. ZrC could be a good replacement material due to its high melting point at high carbon stoichiometries.[2]

2.1 CRYSTAL STRUCTURE

Zirconium carbide (ZrC_x) is a group IV-V transition metal carbide that crystallizes in the rock salt structure, Fm3m structure (space group 225).[17,18] A representation of the ZrC_x crystal structure is depicted in Figure 2.1. In the rock salt structure, the Zr atoms form a metallic face-centered cubic (FCC) structure with the C atoms filling in the interstitial octahedral sites. The crystal structure has a combination of

ionic, covalent, and metallic bonds. The ionic bonds in ZrC arise because of the difference in electronegativity between the C and Zr atoms, covalent bonding occurs from the interactions between the 2p state of carbon and the 4p state of Zr, and the metallic bonding is due to the ionized atoms, causing positive Zr atoms and delocalized electrons that move through the lattice freely.[19] The mixture of bonding gives ZrC_x a unique mixture of properties including its high melting temperature, (~3550 °C), high hardness (~20 GPa), good thermal conductivity ($\geq 10 W m^{-1} K^{-1}$), and good electrical conductivity ($\sim 200 \times 10^4 \Omega^{-1} m^{-1}$).[10,20]

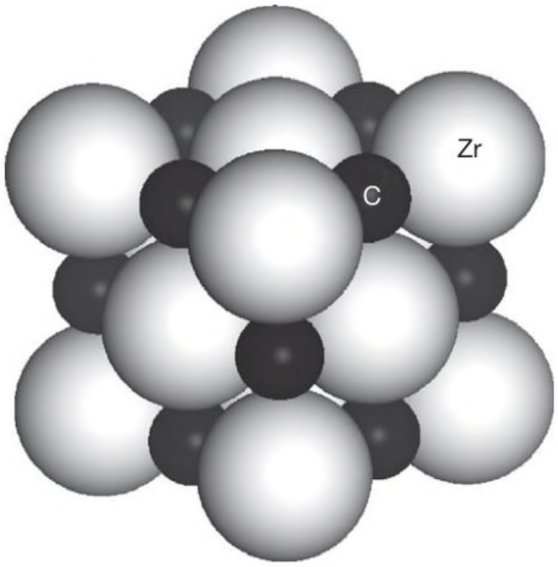

Figure 2.1. ZrC_x rock salt crystal structure.[18]

ZrC_x deviates from its stoichiometric composition by forming vacancies in the carbon sublattice. The range of stoichiometry (C/Zr ratio) can be from ~0.6 to 1, as is shown in Figure 2.2.[21]

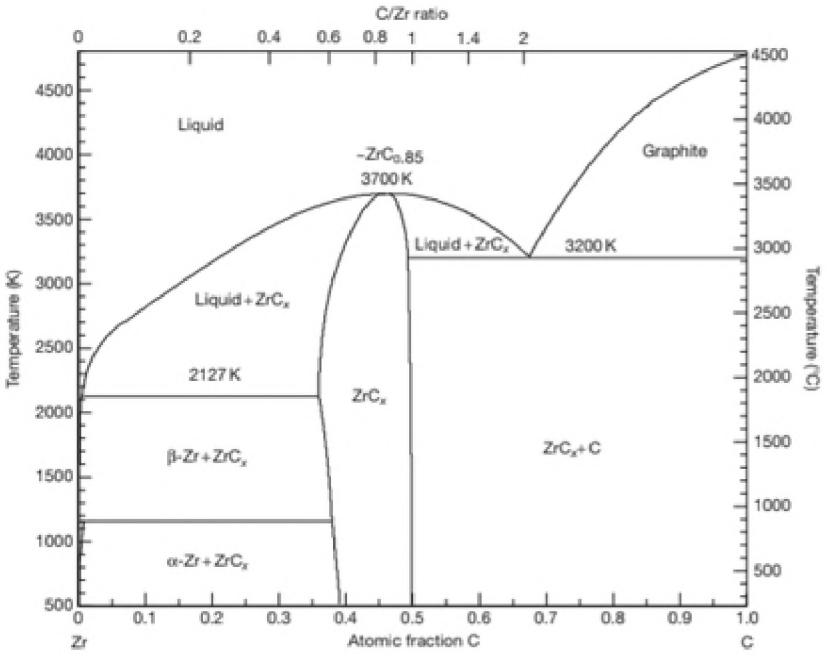

Figure 2.2. The zirconium-carbon phase diagram.[21]

The ZrC_X lattice parameter changes based on the carbon stoichiometry. Equation 1 is a model based on literature values, shown in Figure 2.3, of impurity content, where *a* is the lattice parameter, *x* is the C/Zr atomic ratio, and *y* is the (O + N)/Zr atomic ratio. Overall, the presence of oxygen in the lattice is shown to decrease the lattice parameter.

$$a_{ZrCx(ON)y} = 4.5621 - 0.2080x^2 + 0.3418x - 0.80y(1 - x) \quad (1)$$

Figure 2.3 shows a fit of a parabolic curve in the lattice parameter with respect to the C/Zr ratio from Jackson et al.[18] The peak in the lattice parameter is due to a competing influence between increasing carbon content and increased bond strength up to a C/Zr ratio of about 0.85. The lattice expands with increasing carbon content due to more space needed for interstitials, but at a ratio of 0.85 the lattice contracts with greater carbon content due to increased bond strength.[18] In carbon rich ZrC the lattice parameter

does not significantly depend on the C/Zr ratio due to the precipitation of excess carbon when the ratio exceeds 0.98.[22] Oxygen also has an effect on the lattice parameter. Oxygen replaces more than one carbon atom thereby decreasing the lattice parameter.[23] If oxygen content is not measured, basing the carbon content on the lattice parameter alone will result in incorrect values.

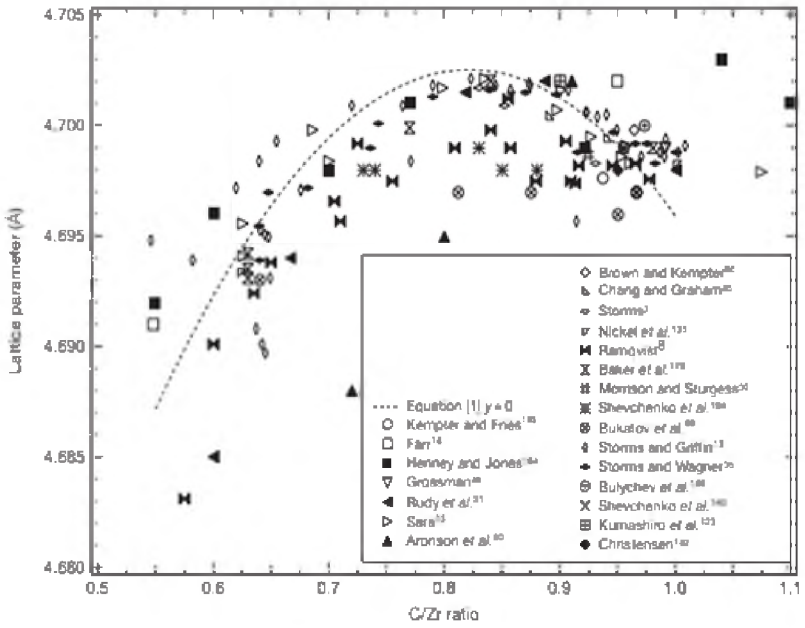

Figure 2.3. Lattice parameter of ZrC as a function of the C/Zr ratio.[18]

2.2 PROCESSING OF ZIRCONIUM CARBIDE CERAMICS

ZrC_x can be produced in a variety of ways and various fabrication techniques that can provide varying characteristics to samples including microstructure, chemical composition, and impurity concentrations. The methods to produce ZrC_x include solid phase reactions, solution-based precursors, and vapor phase reaction methods.

2.2.1 Solid Phase Reaction. Carbothermal reduction of ZrO_2 powders by C has historically been the most common synthesis route used to obtain ZrC, this method is commonly used for commercially available ZrC powders.[24] This method requires high temperatures for long dwell times to obtain high purity ZrC_x powders. The reaction requires a strictly controlled atmosphere (vacuum or inert gas) to ensure the final purity of the ZrC_x. Due to the way this reaction propagates, with the C diffusing into the ZrO_2, the formation of ZrC is highly localized.[25] The ZrO_2 and C powders need to be well mixed and dispersed together to ensure a compete reaction. The carbothermal reduction often results in the formation of an oxycarbide ZrC_xO_y due to carbon deficiencies and the solubility of oxygen in zirconium carbide.[26] The carbon sublattice can have a large number of vacancies and the oxygen impurities usually sit in those vacancies. The oxygen impurities can influence densification and thermomechanical properties in ZrC_x ceramics.[27]

Through the "Reaction" module calculations in FactSage 7.2, it was determined that this carbothermal reduction is endothermic and favorable above 1100 °C under mild vacuum (~150 mTorr). The total reaction, shown in Equation 2, can be split into two steps, Equations 3 and 4. The first reaction is zirconia and carbon reacting to form a zirconium oxycarbide, and in the second step the oxycarbide reacts with the remaining carbon to form ZrC.

$$ZrO_{2\,(s)} + 3C_{(s)} = ZrC_{\,(s)} + 2\,CO_{\,(g)} \quad (2)$$

$$ZrO_{2\,(s)} + C_{(s)} \rightarrow ZrC_xO_{y(s)} + CO_{(g)} \quad (3)$$

$$ZrC_xO_{y(s)} + C_{(s)} \rightarrow ZrC_{\,(s)} + CO_{\,(g)} \quad (4)$$

Another solid phase method is the combustion synthesis reaction. This reaction is a direct reaction of C with Zr (Equation 5) or ZrH_2 (Equation 6). It is often used in cases where higher purity or controlled carbon stoichiometry is desired. The combustion method consists of heating up a pressed green body to a temperature known as an ignition temperature after which heat is released. The heat released from the reaction is enough to sustain the reaction to completion as long as the particles are in contact. This reaction is so energetic that green bodies can break apart if there is not an external confinement pressure. Methods that utilize ZrH_2 to form and densify ZrC in one furnace run, reduce possible oxygen impurities by preventing the formation of surface oxides that occur during handling of the powder between the reaction furnace and the hot press. Two major benefits of the hydride method are the lower reaction temperature and less carbon required to complete the reaction. While ZrC can be formed at lower temperatures using this method, oxygen also tends to remain in the lattice. To remove the oxygen in the lattice, higher temperatures are required.[28]

$$Zr_{(s)} + C_{(s)} = ZrC_{(s)} \quad (5)$$

$$ZrH_{2(s)} + C_{(s)} = ZrC_{(s)} + H_{2(s)} \quad (6)$$

The hydride-based route, in which ZrH_2 is reacted with a carbon source transitions from exothermic to endothermic at approximately 925 °C. This reaction is favorable even at room temperature, as determined from FactSage 7.2 "Reaction" module calculations. The metallic Zr reaction is favorable at all temperatures.

With the reactive route, a greater range of stoichiometries can be prepared and the time to reaction completion is lower compared to the carbothermal reaction method. Sub-stoichiometric C/Zr ratios, which are difficult to prepare via carbothermal reduction due

to the abundance of oxygen and zirconia remaining in synthesized ZrC, are more easily synthesized with the hydride route. During reaction ZrH_2 readily decomposes when heated resulting in reactions of ZrH_2 and metallic Zr likely reacting together as the system is heated. While a purer product can be made with the combustion reaction there are issues in using this method for bulk production of ZrC_x. The two main issues are the exothermic nature of the reaction and the zirconium reactant being highly pyrophoric and susceptible to oxidation.

2.2.2 Solution-Based Fabrication. Solution-based precursors can be used to synthesize ZrC_x.[2,19] The solution-based method allows for increased mixing on a molecular scale. This increased mixing makes for a more efficiently diffused reaction allowing for decreased temperature and time for the reaction. The most common solution-based route for the production of ZrC_x powders is Sol-gel processing. Most commonly Zr n-propoxide or zirconium oxychloride and a carbon source, such as alcohol or sugar, are used to produce a polymer containing Zr-O-Zr links. The final product is separated from the solvent by drying and then is carbothermal reacted. Most solution-based routes make ZrO_2 that has to undergo carbothermal reduction to make ZrC. Varying stoichiometries of ZrC_x can be achieved using different proportions of the reactant precursors. The solution-based method also has the disadvantage of residual oxygen impurities.

2.2.3 Vapor Phase Fabrication. Producing ZrC_x using vapor phase reactions is mainly used to create coatings, and is the most common method used for nuclear fuel coatings. The high melting temperature of ZrC_x causes the coatings to be deposited by vapor phase deposition such as chemical vapor deposition (CVD), evaporation, or sputtering.[1,29,30] For the nuclear fuel concept, such as Tri-structural Isotropic (TRISO) fuel particles, the preferred method is CVD to produce high purity, uniform, and defect free ZrC coatings onto the particles. The process that is used is reacting a zirconium halide with a gaseous hydrocarbon compound such as methane (CH_4) at temperatures between 1300 and 1500°C to produce a gaseous ZrC which is then deposited on a suitable substrate. Several zirconium halides have been used in this method including chloride, iodide, and bromide. The process can be shown by the reaction below.

$$ZrX_4 + CH_4 + 2(1 - x)\,H_2 \rightarrow ZrC_x + 4HX \; (X = Cl, I, Br, x \leq 1) \qquad (7)$$

The reaction takes place in a controlled inert environment to avoid gaseous impurities such as oxygen from being included in the final product. This CVD method can also produce varying stoichiometries of ZrC_x by controlling the flow of CH_4 and hydrogen. After deposition, heat treatments can be used to achieve reasonable densities of the coatings.

2.3 SINTERING AND DENSIFICATION

Densification of ZrC is difficult and often requires sintering temperatures above 2000°C. There are a few densification methods that have been used to densify ZrC_x including pressureless sintering, hot pressing, reactive hot pressing, and spark plasma sintering.

In addition to the varying densification methods. To aid in densification, sintering aids are often added. These sintering aids are usually a Zr source and/or a C source, such as a metallic zirconium, ZrH_2, or graphite.[11,31] In addition to improving densification, Zr-containing sintering aids can also be used to enable controlled reductions to define the C/Zr ratio. This technique has been used with additions of both Zr and ZrH_2 to produce near-stoichiometric ZrC before hot-pressing.[11,31] In the case of C-containing sintering aids, the benefit is balanced between the two effects. Additions of extra carbon increase densification through the removal of surface oxides on prepared powders, but decrease densification due to the reduction in carbon vacancies.[31] A comparison of the same hot-pressing schedules used for varying ZrC compositions shows that increased carbon vacancies decreased the C/Zr ratio and increased the final density of the resulting ZrC_x ceramic, shown in Table 2.1.

After the carbothermal reduction, the prepared ZrC powder undergoes final densification to form bulk ZrC. Densification of ZrC is easier at lower C/Zr ratios due to increased carbon vacancies which enhance carbon mobility.[32]

Table 2.1. Effects of C/Zr ratio on densification of ZrC ceramics during hot pressing.

Composition	Grain Size (μm)	Temperature (°C)	Pressure (MPa)	Relative Density (%)	Reference
ZrC	3.7 ± 1.3	2100	30	91.9	Wei et al.[11]
$ZrC_{0.9}$	30.6 ± 10.8	2100	30	97.3	
ZrC	-	2000	30	83	Wang et al.[31]

2.3.1 Pressureless Sintering. Few studies have involved the pressureless sintering of ZrC due to the difficulty in densifying without additives or extensive high-energy milling. Silvestroni et al. pressurelessly sintered ZrC with up to 20 vol% $MoSi_2$ additions at 1950°C for one hour.[33] The ZrC without additives reached a final density of ~73% compared to the ZrC with 20 vol% $MoSi_2$ which reached a final relative density of ~97% at 1950°C. Zhou et al. used high-energy ball milling, as well as additives, to help densify ZrC.[34] The high-energy ball milling had a great effect on the final density, the milled ZrC had a final relative density of ~86% at 1900°C and ~98% at 2100°C, dwell times were two hours . Schönfeld et al. sintered ZrC at temperatures ranging from 1850 – 2000°C with varying carbon stochiometries.[35] Batched, stoichiometric ZrC achieved a maximum relative density of ~86% at 2000°C, while lowering or raising the carbon content increased the density to above 95%. Sacks et al. utilized nanocrystalline ZrC powders to obtain relative densities of ~99%.[36] Sacks et al. also used a two-step sintering process wherein the ZrC was "pre-sintered" at 1600°C for two hours and then fully sintered at temperatures up to 1950°C for an additional two hours. In order to pressurelessly sinter ZrC, high temperatures at extended dwell times are needed to obtain densities above 90%. The high temperatures required can be lowered using a sintering aid or with a decrease in the starting powder particle size.

2.3.2 Hot Pressing. Hot pressing is the most conventional method used in the densification of ZrC_x. During hot pressing, the powder is densified using high temperatures and applying an external pressure. Wang et al. hot pressed ZrC at 1900°C under a 30 MPa applied pressure for one hour, resulting in a relative density of 80%.[17] Applying pressure increased density by ~6% from the pressureless sintering processed

used by Silvestroni et al. at a lower temperature. Wang et al. basically showed that ZrC could achieve a relative density of ~ 92% by hot pressing at 2000°C without additives or high energy milling. Shen et al. hot pressed ZrC at 1900 and 2000°C for one hour under a 30 MPa pressure and achieved relative densities of ~94 % and ~95%, respectively.[37] The increase in density from Weng et al. to Shen et al. can be attributed to the decrease in particle size of the ZrC in Shen et al.. ZrC Hot pressing lowers the dwell time required at high temperatures compared to pressureless sintering.

2.3.3 Reactive Hot Pressing. Reactive hot-pressing (RHP) allows for densification at lower temperature than the traditional hot-pressing method and carbothermal route. This is due to synthesis reactions and sintering taking place concurrently, as opposed to just sintering a pre-reacted material. Nachiappan et al. used RHP to produce ZrC by using zirconium metal and graphite as the starting materials.[38] The starting powders underwent RHP for 30 minutes using a 40 MPa pressure at varying temperatures (1200 to 1600°C) and over a range of compositions. The stoichiometric samples did not get more than 85% dense. The sub-stoichiometric samples densified up to 99% relative density after heat treatment at 1800°C for one hour, while those without the heat treatment contained unreacted starting material. Rangaraj et al. used Zr and graphite reactants for RHP at 1200°C for one hour and obtained densities up 93% and 99% for stoichiometric and sub-stoichiometric ZrC respectively.[39] RHP also occurs when the starting materials are ZrC and ZrH_2. This method will always result in sub-stoichiometric ZrC. Wei et al. performed RHP as a two-step process, reactive sintering and hot pressing, with the first step being performed at 1300°C for 30 minutes then hot pressing up to 2100°C for one hour under a 30 MPa pressure.[11] Densities for their study

were >95% using this method. RHP can lower the sintering temperature compared to conventional hot pressing but RHP requires an additional heat treatment stage to ensure that the stoichiometry is uniform across the sample.

2.3.4 Spark Plasma Sintering. Spark plasma sintering (SPS) has been used to obtain dense materials at lower temperatures and shorter dwell times. Wei et al. obtained 98% relative density for ZrC at 1700°C under a 60 MPa applied pressure and a dwell time of 24 minutes.[40] Specimens with densities above 95% were obtained in as little as 5 minutes of dwell time. Utilizing higher pressures, Sciti et al. performed SPS of ZrC with no additions at 2100°C for 3 minutes under a 65 MPa pressure to obtain a 98% relative density.[13] Further, Jackson et al. obtained a relative density of ~98% from a dwell time of 6 minutes at 2000°C and 70 MPa.[41] SPS has the advantage of shorter dwell times at temperature which minimizes grain growth at the elevated densification temperatures.

2.4 MECHANICAL PROPERTIES

The mechanical properties of ZrC_x at room temperature have been studied with a focus on strength, fracture toughness, and hardness.[5,10,11,13,42] Even with the studies done on ZrC_x, there are some inconsistencies with the values reported in different studies, particularly with strengths ranging from ~220 MPa to ~410 MPa. These differences between studies can be attributed to impurities, vacancies, microstructure, and porosity. Many of the studies reporting these values are not properly characterizing these factors in the literature.

2.4.1 Room Temperature. Elastic modulus for ZrC has been reported in the literature over a range from ~250 to ~400 MPa depending on porosity, stoichiometry, and free carbon.[43] Feng et al. and Wei et al., with near stoichiometric ZrC_x and similar densities, measured the Young's modulus to be 404 ± 11 GPa and 401 ± 13 GPa, respectively.[10,11] Wei et al. also tested sub-stoichiometric $ZrC_{0.6}$ to have a Young's modulus of 255 ± 13 GPa. Work by Chang et al. calculated the polycrystalline elastic modulus of ZrC from single crystal measurements to be 406 GPa.[44]

Room temperature strengths for ZrC_x can vary due to stoichiometry, additives and grain size. In the study by Wei at al., different ZrC_x stoichiometries were densified at different temperatures resulting in grain size differences between the same compositions. For the composition $ZrC_{0.6}$, the strength ranged from ~320 MPa at a grain size of 14 μm to ~220 MPa at a grain size of 62 μm. Shen et al. showed an increase in the strength of ZrC_x from 446 MPa to 512 MPa due to a 5 mol% tungsten additions.[37] Wei et al. shows that overall the strength of ZrC_x decreased with decreasing carbon content.[11]

Fracture toughness of ZrC_x does not appear to vary greatly due to carbon content, as seen in the study by Wei et al. where fracture toughness values were in the range of 2.1 to 2.6 $MPa•m^{1/2}$ and was largely controlled by grain size, smaller grain sizes made the crack path more tortuous enhancing the fracture toughness. Feng et al. reported a fracture toughness of 2.3 ± 0.2 $MPa•m^{1/2}$ and Katoh et al. reported a fracture toughness of 2.7 ± 0.3 $MPa•m^{1/2}$.[2] Fracture toughness for near stoichiometric ZrC_x thus appears to fall around ~2.5 $MPa•m^{1/2}$.

Hardness of ZrC_x varies widely in literature from 12 to 30 GPa. This range is due to stoichiometry, porosity, and hardness indentation load. Many hardness values are

reported without the load used to produce the indents, as well as not reporting the ZrC_x stoichiometry. Sciti et al. reported a hardness of 17.9 GPa under a 1 kgf and 25.2 GPa using a nanoindentation technique.[13] Min-hage et al. reported a hardness of 13 GPa for $ZrC_{0.97}$ without load or grain size being reported.[12]

2.4.2 Elevated Temperature. Few studies have been conducted with respect to the mechanical properties of ZrC_x at elevated temperatures. However, Fedotov et al.. reported strength values for ZrC, under a mild vacuum with a C/Zr of 0.96 and a grain size of 250μm, up 2600°C [45] The strengths of the ZrC reached a maximum at ~200 MPa at 2000°C, an increase over the ~150 MPa strength values at room temperature. Strength then decreased to 40 MPa at 2600°C. Gridneva et. al. measured the strength of ZrC with a C/Zr of 0.95, 2.5% porosity, and a grain size of 10 μm under a mild vacuum up to1800°C.[46] They reported a maximum strength of ~220 MPa at 1000°C, decreasing to ~150 MPa at 1500°C.[46] Gridneva et al. also measured hardness as a function of temperature, where hardness was found to decrease linearly from ~20 GPa at room temperature to ~4 GPa at 1000°C. A study by Leipold et al. found that the mechanical properties at high temperatures were controlled by impurities.[15] Many of the reported elevated temperature mechanical properties are from older studies which generally did not report impurities or the carbon stoichiometry. A more recent study by Shen et al. reported strengths up to 1800°C, measured in flowing argon.[37] The ZrC tested was 94% dense with a grain size of ~ 11 μm. The strengths from 1000°C to 1600°C were about 350 MPa, and then decreasing to ~300 MPa at 1800°C.[37] The increase in strengths from the older studies might be due to a decrease in impurities for the tested ZrC_x, although some studies did not report their impurities.

PAPER

I. PROCESSING AND ROOM TEMPERATURE PROPERTIES OF ZIRCONIUM CARBIDE

ABSTRACT

Zirconium carbide (ZrC) powder, batched to a ratio of 0.98 C/Zr, was prepared by carbothermal reduction of ZrO_2 with carbon black. Nominally pure ZrC powder had a mean particle size of 2.4 μm. The synthesized powder was hot pressed at 2150°C to a relative density of >95%. The mean grain size was 2.7 μm ± 1.4 with a maximum observed grain size of 17.5 μm. The final hot-pressed billets had a C/Zr ratio of 0.92 as determined by gas fusion analysis. The mechanical properties of $ZrC_{0.92}$ were measured at room temperature. Vickers' hardness decreased from 19.5 GPa at a load of 0.5 kgf to 17.0 GPa at a load of 1 kgf. Flexural strength was 362.3 ± 46 MPa, Young's modulus was 397 ± 13 MPa, and fracture toughness was 2.9 ± 0.1 $MPa*m^{1/2}$. Analysis of mechanical behavior revealed that the largest ZrC grains were the strength-limiting flaw in these ceramics.

1. INTRODUCTION

Zirconium carbide (ZrC_x) is stable across a wide range of carbon stoichiometries from x = 0.63 to 0.98, where x is the C/Zr ratio. Zirconium carbide is a material belonging to the ultra-high temperature ceramics (UHTC) class of materials that is characterized by melting temperatures above 3000°C. In addition to its high melting

temperature, (~3550 °C), other properties such as high hardness (~20 GPa), good flexural strength (~ 400 MPa), wear resistance, and resistance to nuclear fission product corrosion make ZrC_x of interest for use in extreme environments.[1,2] These properties make ZrC_x useful for high-speed tooling, hypersonic vehicles, rocket nozzles, and nuclear reactor core materials.[3–8]

The processing and mechanical properties of ZrC_x have been reported.[1,9–11] Densification is difficult due to strong covalent bonds and low self-diffusion rates.[8] To densify ZrC_x, high temperatures and pressures are needed. ZrC_x also gets more difficult to densify with increasing C stoichiometry due to fewer vacancies, resulting in lower plasticity and mass transport rates. To improve the densification of ZrC_x, additions of C, ZrH_2, and various transition metal carbides (MC) have been used.[2,9,12] Sintering additives can, however, change the ZrC_x stoichiometry and microstructure. ZrH_2 additives lower the stoichiometry of the ZrC_x, producing more vacancies that allow for increased movement within the structure and result in improved densification. However, ZrH_2 also generates increased grain growth at higher temperatures.[9] Additions of C improve densification by reducing the oxide impurity content on the surface of the powder particles that inhibits densification. Removal of surface oxides increases sinterability while unreacted carbon reduces grain growth by grain pinning.[12] In addition to approaches that use additives, reactive hot pressing (RHP) has been used to produce dense ZrC ceramics. RHP decreases the densification temperature and allows for deformation of the ZrH_2, after H_2 volatilization but before reacting with C to form ZrC.[13]

Not many studies have reported the effects of C stoichiometry and impurities on the mechanical properties of ZrC_x. Lower C stoichiometry seems to decrease the hardness

of ZrC.[9] Further, small quantities of Hf (a few atomic percent) are present in all Zr resources in nature, and the presence of Hf has been reported to decrease thermodynamic properties in ZrB_2.[14,15]

The objective of the present study was to investigate the room temperature mechanical properties of low impurity, including low Hf, near stoichiometric ZrC_x.

2. EXPERIMENTAL PROCEDURE

2.1 PROCESSING

The precursor powders used in this study were ZrO_2 (Materion, Mayfield Heights, OH) and carbon black (N110, J. M. Huber Corporation, Edison, NJ). The ZrO_2 had a reported purity of 99.7 wt% with a reported particle size of less than 45 μm and Hf content of 0.0026 wt%. The ZrO_2 was attrition milled for one hour (Model HD-01, Union Process, Akron, OH) with 3 mm spherical yttria stabilized ZrO_2 media to reduce particle size, after which point the average particle size of the attrition milled ZrO_2 was 2.3 μm. The carbon black powder had an average size of 0.38 μm. The powders were batched to a molar ratio of C/Zr = 0.98. The batched powders were ball mixed for 4 hours in acetone with cylindrical yttria stabilized ZrO_2 media in order to obtain a homogenous mixture. The slurry was then dried via rotary evaporation (Rotavapor R-124, Buchi, Flawil, Germany) under mild vacuum at a temperature of 65°C and a rotation speed of 60 rpm. The mixed powder was passed through a 100-mesh sieve to break up any large agglomerates, and then uniaxially pressed into pellets for carbothermal reduction.

The carbothermal reduction occurred in a graphite furnace (3060-FP20, Thermal Technology, Santa Rosa, CA) and the pressed pellets were placed in a graphite crucible. The pellets were heated at 10 °C/ min under vacuum (~150 mtorr) to 1800°C and held at temperature for 4.5 hours. This reaction temperature was chosen to promote removal of residual oxygen from the ZrC lattice. The reacted powder was ball mixed for 4 hours in acetone with ZrO_2 media to break up the pellets. The powder was dried and passed through a 100-mesh sieve. The average particle size of the reacted powder was 2.4 μm.

The reacted powder was hot-pressed in a 47 mm x 31 mm rectangular graphite die lined with graphite foil and coated with boron nitride. The graphite die was loaded into a hot press (HP20−3060-20; Thermal Technology, Santa Rosa, CA) and heated at 25°C/min to 1600°C, with a one hour hold under mild vacuum (~150 mtorr), and then heated to 1650°C and held for 10 minutes. The holds were used to remove any surface oxides on the powder surfaces resulting from exposure to the air after reaction of the powder. After the 1650 °C hold, the furnace was backfilled with helium and a uniaxial pressure of 32 MPa was applied. The temperature was then increased at a rate of 50 °C/min to 2150 °C for the final hot-pressing temperature. The sample was held for 35 min at 2150 °C. After the 35 min hold, the furnace was cooled at a rate of 45 °C/min to 1600 °C. At that temperature, the uniaxial pressure of 32 MPa was removed. From 1600 °C the furnace was allowed to naturally cool to room temperature.

2.2 CHARACTERIZATION

The density of the hot-pressed billets was measured using a modified Archimedes' method. The billets were placed in distilled water and boiled for two hours,

then placed under mild vacuum for 30 minutes before measurement. Scanning electron microscopy (SEM; Raith eLine) was used to examine microstructures. To prepare the specimens for microscopy, the reaction layer on the outside of the billets was removed and a cross section was taken from the billet followed by polishing to a 0.25 μm finish using successively finer diamond abrasives. The resulting polished specimens were thermally etched at 1600 °C for 30 minutes to increase the visibility of the grain boundaries. A low voltage of 5kV was used to increase orientation contrast. The grain size was determined from SEM images using ImageJ software (National Institutes of Health, Bethesda, MD). The grain size was averaged from over 1000 grains using Feret's diameter. X-ray diffraction (XRD; X'Pert Pro, PANalytical, Almelo, Netherlands) analysis was used to identify the phases in the finished hot-pressed billets. The billets were crushed and ground with a zirconia mortar and pestle, then passed through a 200-mesh sieve. Diffraction patterns were obtained by scanning from 15-138° two theta using a step size of 0.03°, an effective scan step time of 9.8 minutes. Carbon stoichiometry and oxygen content were measured via the gas fusion method using oxygen (TC 500, LECO, St. Joseph, MI) and carbon (CS 600, LECO) analyzers. Raman spectroscopy (Aramis Labram, Horiba Jobin Yvon, Edison, NJ) was performed with a He-Ne laser, no filter, a hole size of 500 μm, and a slit size of 150 μm at 50x magnification. The Raman spectrums were obtained from 200 to 2000 wavenumber (cm^{-1}) with a 15 second acquisition time, averaging three acquisitions for each scan.

2.3 MECHANICAL TESTING

Billets were cut into bars by electrical discharge machining (EDM: AgieCut HSS150, GF Manufacturing Technology, Switzerland). After cutting, the sides of the bars that were in contact with the EDM wire were surface ground (FSG-3A818, Chevalier, Santa Fe Springs, CA) to remove any damage from the wire cutting. Bars for testing flexure strength and fracture toughness were cut to 3 mm x 4 mm x 45 mm, which are size B-bars according to ASTM C1161. The tensile surface of the bars was then ground using a 600-grit diamond grinding wheel then chamfered and hand polished to a 0.25 μm surface finish. Testing used a crosshead rate of 0.50 mm/min, and five bars were tested for flexure strength. Fracture toughness was determined by chevron notch testing (ASTM C1421), with six bars tested. A chevron notch was machined into the bars with a pneumatic saw (Accu-cut 5200, Aremco Products, Ossining, NY). The bars were tested using an instrumented load frame (Instron 5881, Instron, Norwood, MA). For fracture toughness, a preload of around 60 N was oscillated three times before breaking the bars. After breaking the bars in the first test, the two halves from each bar were notched again for further testing in an ASTM C1161 A-bar fixture. The dimensions of the notches were measured after testing using a digital optical microscope. Hardness was measured by Vickers indentation (ASTM C1327), with two different indentation loads, 9.81 N and 4.91 N, and a dwell time of 10 seconds each, with 10 indents for each load per specimen. A lighter load was used due to higher loads causing a large amount of spalling around the sides of the indents. Dynamic elastic and shear moduli were determined using impulse excitation (ASTM 1259). The static elastic modulus was also measured from the four-

point bending tests, using the measured deflection at the center of the beam and assuming that the bottom load train was more rigid than the specimen.

3. RESULTS AND DISCUSSION

3.1 DENSITY AND MICROSTRUCTURE

Single phase ZrC_x was formed by hot pressing. The diffraction peaks were indexed to ZrC using powder diffraction file (PDF) 01-073-0477 as shown in Figure 1. ZrC_x has a rock salt structure and all of the peaks were indexed to ZrC with no unindexed peaks. The material appears to be single phase ZrC by XRD.

The hot-pressed ZrC_x was near fully dense with a uniform grain size. The relative densities were >95% for all tested billets. The average grain size of the hot-pressed ZrC_x was 2.7 ± 1.4 μm with a maximum observed grain size of 17.5 μm. SEM analysis of the microstructure, as shown in Figure 2, was consistent with density measurements, revealing ~4% porosity for hot-pressed specimens. Most of the porosity in the billets was intragranular porosity. Porosity appeared in SEM images as black circles with charging around the edges. In addition, a second black phase with no charging was observed, which is consistent with the presence of carbon inclusions. The pores and the secondary phase are isolated and smaller than the grain size, indicating that they should not affect the strength of the material.

The second black phase was identified as carbon with Raman spectroscopy. The peaks shown in Figure 3 are from carbon with the peak at ~1350 cm^{-1} referred to as the disorder-induced (D) peak and the peak at ~1582 cm^{-1} referred to as the graphite (G)

peak. Fully ordered graphite only has one peak, the G peak. The G peak relates to the in-plane stretching mode of graphite and the D peak is related to a double resonance in disordered carbon.[16] Dash et al. observed similar carbon inclusions using TEM and revealed that the inclusions were made of a network of graphite ribbons.[16] The ZrC in the present study was produced by carbothermal reduction in a graphite furnace and hot-pressed in a graphite furnace and die. The carbon present as a second phase could either be unreacted carbon from the initial batch or due to interactions with the furnace or hot press. The total carbon content of the hot-pressed billets was measured using carbon analysis. The calculated carbon to zirconium ratio was 0.92. Oxygen analysis identified the oxygen content to be below 0.5 wt% for all samples. Varying levels of C and O in the ZrC structure change the lattice parameter, increasing the lattice parameter with increasing C content.[17] The lattice parameters for the specimens averaged 4.6945 Å. This lattice parameter is close to the C-rich values reported by Réjasse et al.[17] Calculating the C/Zr ratio with the equation from Réjasse et al., and the lattice parameter measured using XRD in the present study, resulted in a predicted C/Zr molar ratio at 0.94, which is equivalent to $ZrC_{0.94}$. This number is different from the ratio calculated using carbon analysis, which is likely due to the presence of some oxygen dissolved onto carbon vacancies in the lattice, which resulted in a lattice parameter matching more closely to the more C rich specimens of Réjasse et al..

3.2 MECHANICAL PROPERTIES

Mechanical properties for the $ZrC_{0.92}$ produced in this study were tested at room temperature, and the results are summarized in Table 1. Dynamic measurements of

modulus resulted in a Young's modulus of 397 ± 13 GPa and a shear modulus of 161 ± 4 GPa. The static, average Young's modulus, measured in four-point bending was slightly lower, at 371 ± 12 GPa. The slightly lower value for the static measurements is not surprising, given the potential for load train compliance issues with these types of measurements. The modulus value measured using impulse excitation falls within reported values in the literature for similar C/Zr ratios.[9,18] Vickers hardness was 17.0 GPa when measured using a load of 1 kgf and 19.5 GPa for a load of 0.5 kgf. A lower load was used due to spalling around some indents when higher loads were used. Hardness for ZrC_x has been reported from about 20 to 34 GPa.[18] Hardness can be affected by porosity, C/Zr ratio, and load. For similar compositions, Vickers hardness measured at 1 kgf has been measured to be 17.9 GPa[9,11]. Lower loads around 0.5 kgf increased the hardness to around 20 GPa[19] and nanoindentation has measured hardness values in the range of 25 to 30 GPa[7,11] Based on the porosity, C/Zr ratio, and the loads used, the hardness values for the ZrC in this study fall within the values reported in other studies.

Flexural strength was measured at 362 ± 46 MPa. The measured strength is greater than values from previous studies, which have been in the range of 100-300 MPa[18,1]. The higher strength in the present study can be attributed to lower levels of porosity and smaller grain sizes compared to the other studies. For the reported strengths of around 100 MPa, the grain size was ~50 μm and porosity was 9%.[46] Strengths measured in three-point bending range from 370 to 407 MPa,[9,11] which are similar to values from the present study, although three-point bending should provide higher values than the four-point bend tests in the current study, given a similar critical flaw size. The average fracture toughness was 2.9 ± 0.1 $MPa \cdot m^{1/2}$. Literature values for fracture

toughness range from 2.3 ± 0.2 MPa•$m^{1/2}$ to 2.7 ± 0.3 MPa•$m^{1/2}$.[1,4] The current study values fall within the standard deviation of values found in the literature.

The critical flaw size was estimated using a Griffith type failure analysis. The crack geometry constants were assumed to be Y=1.59 or Y=1.99, which are both used for semi-elliptical surface cracks. Using the average strength and fracture toughness values from the present study, the calculated flaw size was in the range of 16 to 25 μm. From microstructure analysis, the largest grain size that was observed was 17.5 μm. Hence, the likely critical flaw is consistent with the size of the largest grains in the microstructure.

4. SUMMARY

Near stochiometric zirconium carbide with minimal impurities was produced using carbothermal reduction. Ceramics were hot-pressed to relative densities of 95% or greater at 2150 °C for 35 minutes in a flowing helium atmosphere. The average grain size achieved was 2.7 ± 1.4 μm with a maximum grain size of 17.5 μm. The flexural strength was 362 MPa. Young's modulus was between 397 and 371 GPa, based on dynamic vs. static modulus measurements, respectively. Fracture toughness was ~2.9 MPa•$m^{1/2}$. The largest grains in the microstructure were determined to be the critical flaw in four-point bending.

ACKNOWLEDGEMENTS

This research was supported by the National Science Foundation through grant number DMR-1742086.

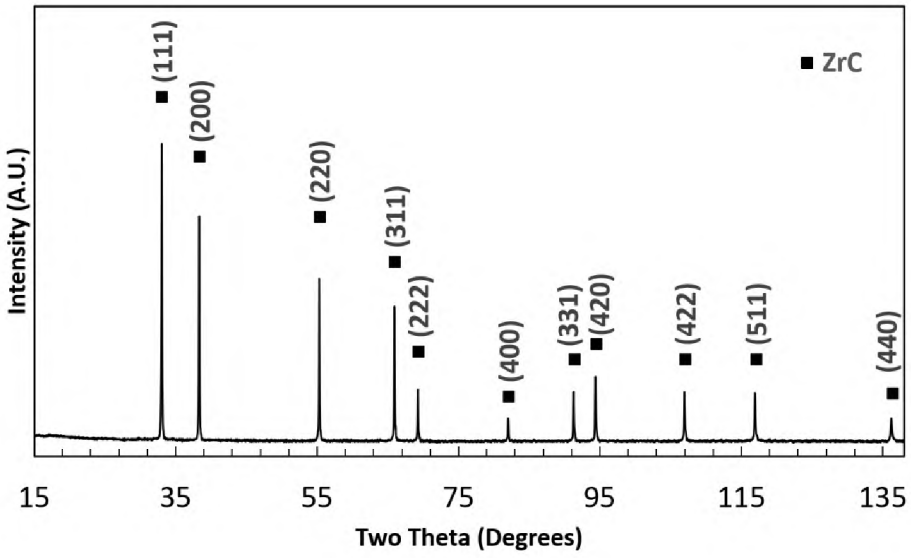

Figure 1. XRD pattern of hot-pressed ZrC indexed to the rock salt structure.

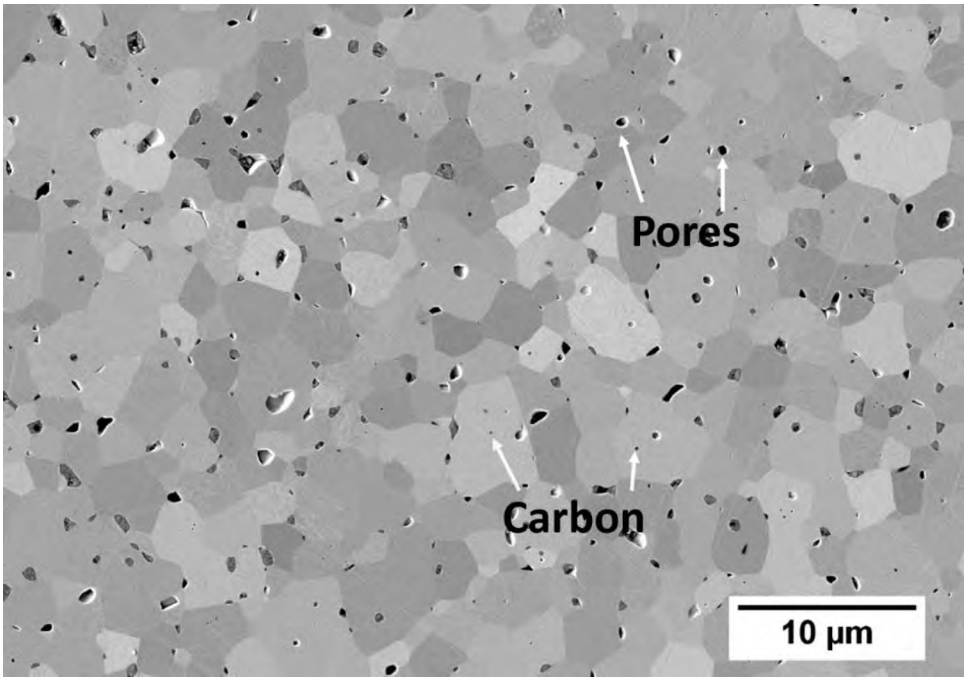

Figure 2. SEM micrograph of a polished cross section of hot-pressed ZrC.

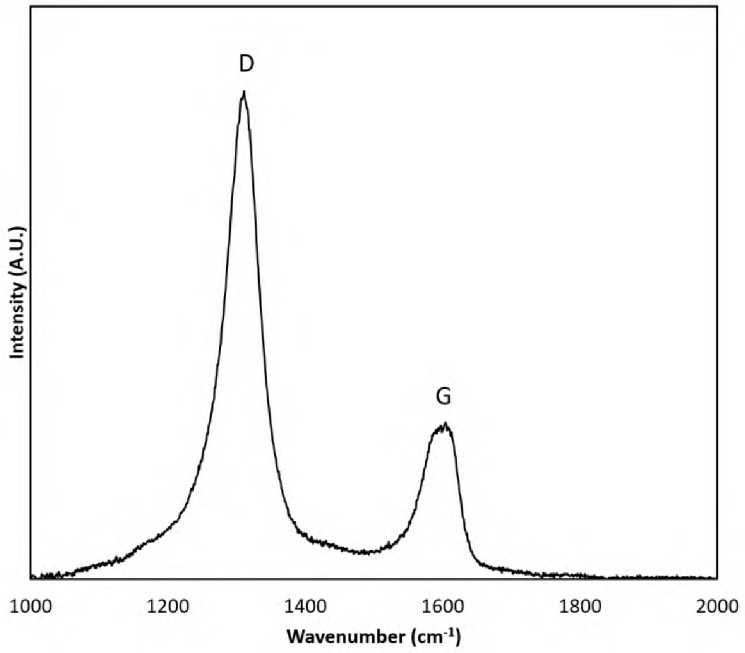

Figure 3. Raman spectrum of the dark inclusions within ZrC_x grains.

Table 1. Summarized mechanical properties of $ZrC_{0.92}$.

Composition	Relative Density (%)	Grain Size (μm)	Young's Modulus (GPa)	Shear Modulus (GPa)	Hardness (GPa)	Flexural Strength (MPa)	Fracture Toughness ($MPa \cdot m^{1/2}$)
$ZrC_{0.92}$	95.9	2.7 ± 1.4	397 ± 13	161 ± 4	17.0 – 19.5	362 ± 46	2.9 ± 0.1

REFERENCES

1. Feng L, Fahrenholtz WG, Hilmas GE, Watts J, Zhou Y. Densification, microstructure, and mechanical properties of ZrC–SiC ceramics. J Am Ceram Soc. 2019;(102):5786–95.

2. Wang X-G, Liu J-X, Kan Y-M, Zhang G-J. Effect of solid solution formation on densification of hot-pressed ZrC ceramics with MC (M = V, Nb, and Ta) additions. J Eur Ceram Soc. 2012;32(8):1795–802.

3. Wang Y, Liu Q, Liu J, Zhang L, Cheng L. Deposition mechanism for chemical vapor deposition of zirconium carbide coatings. J Am Ceram Soc. 2008;91(4):1249–52.

4. Katoh Y, Vasudevamurthy G, Nozawa T, Snead LL. Properties of zirconium carbide for nuclear fuel applications. J Nucl Mater. 2013;441(1–3):718–42.

5. Gosset D, Dollé M, Simeone D, Baldinozzi G, Thomé L. Structural evolution of zirconium carbide under ion irradiation. J Nucl Mater. 2008;373(1–3):123–9.

6. Vasudevamurthy G, Knight TW, Roberts E, Adams TM. Laboratory production of zirconium carbide compacts for use in inert matrix fuels. J Nucl Mater. 2008;374:241–7.

7. Vasudevamurthy G, Katoh Y, Aihara J, Sawa K, Snead LL. Microstructure and mechanical properties of heat-treated and neutron irradiated TRISO-ZrC coatings. J Nucl Mater. 2015;464:245–55.

8. Fahrenholtz WG, Wuchina EJ, Lee WE, Zhou Y. Ultra-high temperature ceramics: materials for extreme environment applications. Hoboken: John Wiley & Sons; 2014. p. 361–415.

9. Wei B, Chen L, Wang Y, Zhang H, Peng S, Ouyang J, et al. Densification, mechanical and thermal properties of ZrC1 − x ceramics fabricated by two-step reactive hot pressing of ZrC and ZrH2 powders. J Eur Ceram Soc. 2018;38(2):411–9.

10. Min-haga E. Sintering and. mechanical properties of ZrC-ZrOa composites. J Mater Sci. 1988;23(1988):2865–70.

11. Sciti D, Guicciardi S, Nygren M. Spark plasma sintering and mechanical behaviour of ZrC-based composites. Scr Mater. 2008;59(6):638–41.

12. Wang X-G, Guo W-M, Kan Y-M, Zhang G-J, Wang P-L. Densification behavior and properties of hot-pressed ZrC ceramics with Zr and graphite additives. J Eur Ceram Soc. 2011;31(6):1103–11.

13. Nachiappan C, Rangaraj L, Divakar C, Jayaram V. Synthesis and densification of monolithic zirconium carbide by reactive hot pressing. J Am Ceram Soc. 2010;93(5):1341–6.

14. Lonergan JM, McClane DL, Fahrenholtz WG, Hilmas GE. Thermal Properties of Hf-Doped ZrB2 Ceramics. J Am Ceram Soc. 2015;98(9):2689–91.

15. Lonergan JM, Fahrenholtz WG, Hilmas GE. Zirconium diboride with high thermal conductivity. J Am Ceram Soc. 2014;97(6):1689–91.

16. Dash RK, Yushin G, Gogotsi Y. Synthesis, structure and porosity analysis of microporous and mesoporous carbon derived from zirconium carbide. Microporous Mesoporous Mater. 2005;86(1–3):50–7.

17. Réjasse F, Rapaud O, Trolliard G, Masson O, Maître A. Experimental investigation and thermodynamic evaluation of the C–O–Zr ternary system. R Soc Chem. 2016;(102):3757–70.

18. Jackson HF, Lee WE. Properties and Characteristics of ZrC. In: Comprehensive Nuclear Materials. London: Elsevier Science; 2012. p. 339–72.

19. Wei X, Back C, Izhvanov O, Khasanov OL, Haines CD, Olevsky EA. Spark plasma sintering of commercial zirconium carbide powders: Densification behavior and mechanical properties. Materials (Basel). 2015;8(9):6043–61.

20. Gridneva IV, Mil'man YV, Rymashevskii GA, Trefilov VI, Chugunova SI. Effect of temperature on the strength characteristics of zirconium carbide. Powder Metall Met Ceram. 1976;15(8):638–45.

II. ULTRA HIGH TEMPERTURE STRENGTH OF ZIRCONIUM CARBIDE

ABSTRACT

The ultra-high temperature mechanical properties were tested for zirconium carbide (ZrC_x) ceramics produced from powder synthesized by carbothermally reducing zirconia and carbon black in an effort to prepare phase pure ZrC_x and determine its intrinsic properties. Powder was prepared with a carbon stoichiometry of 0.92 and then hot pressed at a temperature of 2150°C at a 32 MPa applied pressure. $ZrC_{0.92}$ compositions having a relative density of at least 95% were machined to produce specimens for mechanical property measurements. The elevated temperature strength, from 1600°C to 2000°C, ranged from 375 MPa to ~340 MPa, decreasing to 283 MPa at 2200°C, and further decreasing to 245 MPa at 2400°C. The $ZrC_{0.92}$ produced in this study showed significant strength retention at temperatures above 2000°C.

1. INTRODUCTION

Zirconium carbide (ZrC_x) is a transition metal carbide that belongs to a class of materials known as ultra-high temperature ceramics (UHTCs). This class of materials is known for having melting temperatures above 3000°C. The high melting temperature and resistance to nuclear fission product corrosion has made ZrC_x a material of interest for use in nuclear reactors.[1–3]

Room temperature properties of ZrC ceramics have been reported extensively,[4,5] but for use in extreme environments elevated temperature testing is needed to determine

if ZrC_x is stable for use in those environments. Few studies have been conducted at elevated temperatures for mechanical properties of ZrC_x. The strength of ZrC_x has been reported up to 2600°C by Fedotov et al..[6] Fedotov et al. tested bars of carburized Zr with a C/Zr ratio of 0.96 and a grain size of 250 μm under a mild vacuum. The strength of the $ZrC_{0.96}$ was ~150 MPa at room temperature, reaching a maximum of ~200 MPa at 2000°C, and decreasing to 40 MPa at 2600°C.[6] Gridneva et al. measured the strength of ZrC up to 1800°C in mild vacuum and reported a maximum strength of ~220 MPa at 1000°C, which decreased to ~120 MPa at 1500°C.[7] Their ZrC had a C/Zr of 0.95, porosity of 2.5%, and an average grain size of 10 μm. A more recent study by Shen et al. reported strengths up to 1800°C in flowing argon, the strengths from 1000°C to 1600°C were about 350 MPa and then decreased to ~300 MPa at 1800°C.[8] The ZrC measured in the study had a density of about 94% and a grain size of 10.9 ± 3.0 μm.[8] In the previous studies, most of the researchers do not list the impurities of C/Zr. In the older studies. the tests at elevated temperature were done only in mild vacuum, probably contributing to greater oxidation of the surface of the bars tested. Further, in most of the previous studies, information about the preparation of the test bars is not provided beyond basic dimensions, and this can have an impact on the strengths.

The purpose of this study is to report the strength of $ZrC_{0.92}$ at elevated temperatures, while also reporting impurities, methods used to prepare and test the bars, as well as post-mortem analysis to determine failure origins.

2. EXPERIMENTAL PROCEDURE

2.1 PROCESSING

ZrO_2 (Materion, Reactor Grade, Mayfield Heights, OH) and carbon black (N110, J. M. Huber Corporation, Edison, NJ) were used as the precursor powders for this study. The ZrO_2 had a reported purity of 99.7 wt%. The ZrO_2 powder had a starting particle size in the range of ~45 μm. After attrition milling the powder for one hour, using 3 mm diameter ZrO_2 milling media in acetone, the particle size was reduced to an average of ~2.3 μm. The average particle size of the carbon black powder was 0.38 μm. The powder used in this study was batched to a molar ratio of C/Zr = 0.98. A homogenous mixture of the batched powders was obtained by ball mixing for four hours in acetone with cylindrical ZrO_2 media. The resulting slurry was dried via rotary evaporation under mild vacuum at a temperature of 65°C and a rotation speed of 60 rpm. The dried powder was then passed through a 100-mesh sieve to break up any large agglomerates, and then uniaxially pressed into pellets for carbothermal reduction.

The carbothermal reduction was accomplished in a graphite furnace. The pressed pellets were placed in a graphite crucible and heated at 10°C/ min under vacuum (~150 mtorr) to 1800°C and held at temperature for 4.5 hours. The reacted pellets were crushed by ball milling for 4 hours in acetone with ZrO_2 media. The powder was dried via rotary evaporation and passed through a 100-mesh sieve. The average particle size of the reacted powder was 2.4 μm, determined using a laser diffraction particle size analyzer (Microtrac S3500, Montgomeryville, PA).

The reacted powder was hot-pressed in a 63.5 mm x 63.5 mm rectangular graphite die lined with graphite foil and coated with boron nitride. The graphite die was loaded

into a hot press and heated at 25°C/min to 1600°C, with a one hour hold under mild vacuum (~150 mtorr), and then heated to 1650°C and held for 10 minutes. The isothermal holds were used to promote removal of oxide impurities from the surfaces of the powder particles. After the 1650°C hold, the furnace was backfilled with helium and a uniaxial pressure of 32 MPa was applied. The temperature was then increased at a rate of 50°C/min to 2150°C for the final hot-pressing temperature. The sample was held for 35 min at 2150°C. After the 35 min hold, the furnace was cooled at a rate of 45°C/min to 1600°C. At that temperature, the uniaxial pressure of 32 MPa was removed. From 1600°C the furnace was allowed to naturally cool to room temperature.

2.2 CHARACTERIZATION

Archimedes' method was used to measure the bulk density of the billets, with an assumed theoretical density of 6.73 g/cm^3. The billets were placed in boiling distilled water for two hours and then placed under mild vacuum for at least 30 minutes to saturate the open pores with water. Scanning electron microscopy (SEM; Raith eLine, Dormund, Germany) was used to examine the microstructures from cross-sectioned specimens produced from the billets from surface grinding (FSG-3A818, Chevalier, Santa Fe Springs, CA) with a 600 grit diamond wheel and polishing with successively finer diamond abrasives to a 0.25 μm surface finish. A low voltage of 5kV was used to increase channeling contrast. Grain size was measured from SEM images using Image J software (National Institutes of Health, Bethesda, MD), using the Feret's diameter. At least 100 grains per specimen were measured to determine average grain sizes. The bars

tested at elevated temperatures were cross sectioned and polished for microscopy using the polishing procedure as outlined above.

2.3 MECHANICAL TESTING

Flexure strengths were measured using four-point bending on polished bars at elevated temperatures from 1600°C to 2400°C following ASTM C1211. Five bars were tested at each temperature to determine the average flexure strength. Hot pressed billets were machined into 3.0 mm by 4.0 mm by 45 mm bars by electrical discharge machining (EDM: AgieCut HSS150, GF Manufacturing Technology, Switzerland). The tensile surface was polished to a 0.25 μm finish using diamond abrasives. The bars were tested using an instrumented load frame (33R4204, Instron, Norwood, MA). The elevated temperature testing was performed in an induction heated environmental chamber under flowing argon. A two-color optical pyrometer, sited on the susceptor, was used to control the temperature. The heating profile used was 100°C/min to each test temperature with a five minute isothermal hold before testing to insure the testing fixture and test specimen had equilibrated. The crosshead rate was 2.5 mm/min, which remained the same across all elevated temperatures.

3. RESULTS AND DISCUSSION

3.1 DENSITY AND MICROSTRUCTURE

Hot-pressed $ZrC_{0.92}$ had a relative density greater than 95%. The average grain size of the hot-pressed billet was 2.7 ± 1.4 μm. SEM analysis of the microstructure,

shown in Figure 1, agrees with the measured density. Porosity was about 4% in the billets which is consistent with the density measurements. About half of the porosity is intragranular. Porosity seen in the SEM images appear as black circles with charging around the edges. The carbon inclusions are seen as black phase with no charging around the edges. The microstructure was the same as the specimens tested in the previous study, with intragranular pores and carbon impurities. As seen in the previous study, the porosity and carbon inclusions are smaller than the grain size and were determined to not be the strength limiting flaw. The room temperature strength reported in the previous study was 362 ± 46 MPa with the strength limiting flaw being the larger grains in the microstructure (~17 μm).

3.2 MECHANICAL PROPERTIES

The room temperature strength is 362 MPa with an increased average strength at 1600°C to 375 MPa. The strengths at room temperature and 1600°C are within the standard deviation of each other. High temperature testing in this study shows that the average strength values, summarized in Table 1, stay relatively consistent at ~350 MPa up to 2000 °C, with strength then decreasing to 283 MPa at 2200°C and 245 MPa at 2400 °C. The strength starts to decrease after 1600°C, similar to what was observed by Shen et al..[37] The strength limiting flaw in the pervious study was the larger grains in the microstructure it is possible that this is also the strength controlling flaw at the temperatures between room temperature and 1600°C. The high temperature strengths are well above some literature reported values, shown in Figure 2.

The strength decreases above 1600°C. The strength decreases at 1800°C to 339 ± 30 MPa, then to 342 ± 32 MPa at 2000°C, to 283 ± 34 MPa at 2200°C, and then to 245 ± 14 MPa at 2400°C. From the results of the current study, the strengths were all above the strength values in the older studies. The combination of porosity, grain size, and decreased impurities all contributed to an increase in strength in this study. The grain size in this study was 2.7 μm, as compared to the grain sizes of Fedotov et al., Gridneva et al., and Shen et al. with grain sizes of 250 μm, 10 μm, and 10.9 μm respectively. The porosity may play a lesser role in the high strengths in the current study. The porosity in Gridneva et al. and Shen et al. was 2.5% and 4.6%, respectively. The oxygen content in this study, compared to other studies, does not show a strong correlation to strength with the older studies having lower oxygen content than current studies. Fedotov et al. and Gridneva et al. measured oxygen impurities of 0.1 wt% and 0.05 wt %, respectively. Shen et al. and the current study measured higher oxygen contents of 0.64 wt% and <0.5 wt%, respectively. While the grain size and impurities might have an impact on the elevated temperature strengths, another possibility that could affect the strength in these older studies is how the bars were processed for mechanical testing. The older studies typically do not mention how the test bars were prepared for testing (e.g., machine, polished etc.), with some studies also not including the testing atmosphere. Fedotov et al. and Gridneva et al. mention testing in a mild vacuum. Shen et al. tested in a flowing argon atmosphere. The other studies do not mention testing atmosphere and this can greatly affect the strengths of the tested materials

The decrease in strength at the higher temperatures might be caused by oxidation of the surface of the test bars, leading to etching of the grain boundaries. With increases

in temperature the test bars were held for longer times at elevated temperatures, this could have increased the oxidation of the surface layer decreasing strength, but this was not studied in detail. In a study by Lanin et al.[9], $ZrC_{0.96}$ was tested, however the processing methods were not mentioned. They observed increases in strength around 1600°C before decreasing at higher temperatures, with the decrease in strength attributed to a relaxation in stress and microplasticity. Shaffer et al.[10] hot pressed ZrC_x at 2250°C under a 14 MPa applied pressure, and they also observed strength increases at higher temperature and attributed these increases to internal stress relaxation. Gridneva et al. did not mention the processing methods used to make their $ZrC_{0.95}$. Gridneva et al. also noted a strength increase at elevated temperatures and attributed it to decreasing porosity and grain size, as well as increasing strength of the grain boundaries. Shen et al. references grain boundary strength as well. At 1800°C the intergranular strength of the hot pressed ZrC_x tested in Shen et al. was weak, resulting in grain sliding and grain pull out.[8] The grain boundaries were strengthened with tungsten additions. They proposed that the tungsten additions decreased the oxygen in the grain boundaries, thus increasing the grain boundary strength. In Shen et al., the high temperature strength at 1600°C is within standard deviation and while the strength at 1800°C is not within standard deviation the decrease from 1600°C to 1800°C is comparable to the current study. Fedotov et al. has a consistent strength up to 1500°C and as seen in the current study a decrease in strength above 2000°C, all of the strengths are >100 MPa lower and this can be attributed to the large grain size of 250 μm. The older studies do not go into detail about how the bars were prepared for strength testing, and since strength is not necessarily a material

property it can be strongly controlled by sample processing. The porosity, impurities, grain size, sample preparation all have an impact on the final strengths.

3.3 SURFACE MICROSTRUCTURE

While the microstructure of the bars tested at elevated temperatures did not change in any statistically significant way, the grain sizes have increased slightly at the higher temperatures, as seen in Table 1. The average grain size increased as the test temperature increased. The room temperature grain size was 2.7 μm increasing at elevated temperatures and reaching a maximum of 4 μm at 2200°C. With this increase in average grain size, the largest grains, which were determined to be the strength limiting flaws, are also likely increasing in size which would result in decreased strengths at elevated temperatures. However, the overall grain size average stayed within the standard deviation of the as hot-pressed grain size. The tensile surface of the of the bars was oxidized and the morphology of the oxide layer changes based on the test temperature, as shown in Figure 3. The surface at 1800°C shows etching preferentially along the grain boundaries. In Shen et al., the decrease in the strength of the grain boundaries of the ZrC_x was attributed to the increased oxygen along the grain boundaries. At temperatures above 1000°C grain boundary diffusion predominates the reaction.[4] At 2000°C there is no visible grain structure any more, more of a uniform, rocky surface. At 2200°C the grain boundaries can be seen again. as well as a large number of pores within each grain. ZrC_x can diffuse oxygen to create an oxycarbide then the oxycarbide will start to precipitate carbon and ZrO_2. At temperatures above 470°C a zirconium oxycarbide surface phase forms which starts to form amorphous ZrO_2 and C, cubic zirconia starts to nucleate

forming an oxide layer with the free carbon stabilizing the cubic zirconia, then oxygen starts to defuse through the oxide layer to the free carbon forming carbon dioxide (CO_2) leaving voids and pores in the zirconia layer.[11] The carbon precipitation could be what is causing the porous microstructure.

4. SUMMARY

Flexure strengths of $ZrC_{0.92}$ were measured up to 2400°C in a flowing argon atmosphere. Relatively dense, ~95%, billets of $ZrC_{0.92}$ with an average grain size of ~3 μm were produced by hot pressing. Strength between room temperature and 1600°C remained fairly constant at ~362 MPa ± 46 MPa, decreasing to ~340 MPa between 1800 and 2000°C, further decreasing at 2200 and 2400°C to 283 MPa and 245 MPa, respectively.

ACKNOWLEDGEMENTS

This research was supported by the National Science Foundation through grant number DMR-1742086.

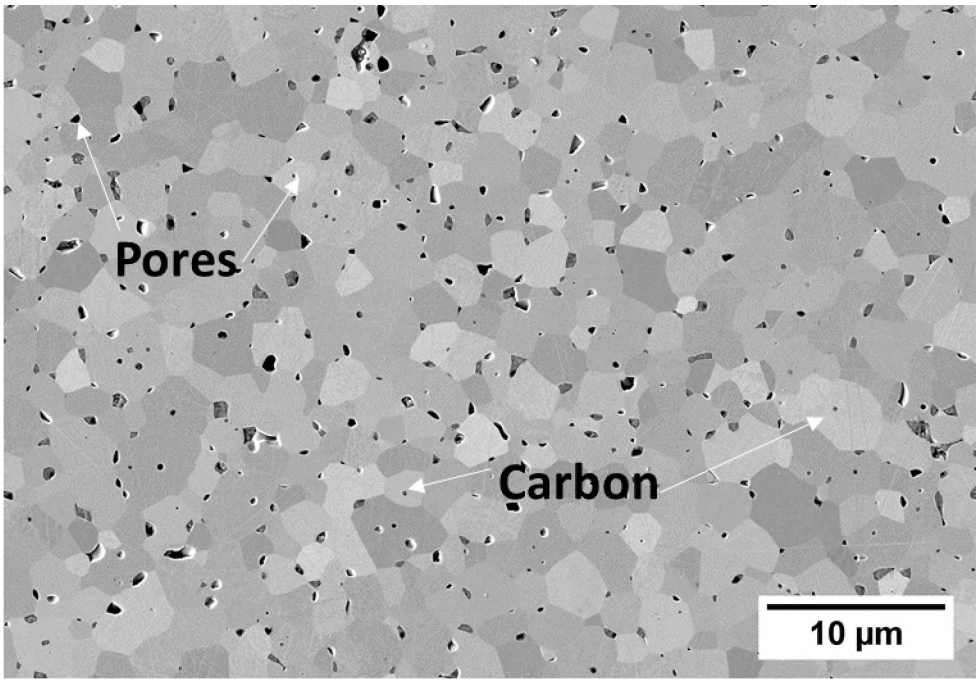

Figure 1. Secondary electron micrograph of a polished cross section of the hot-pressed ZrC ceramic.

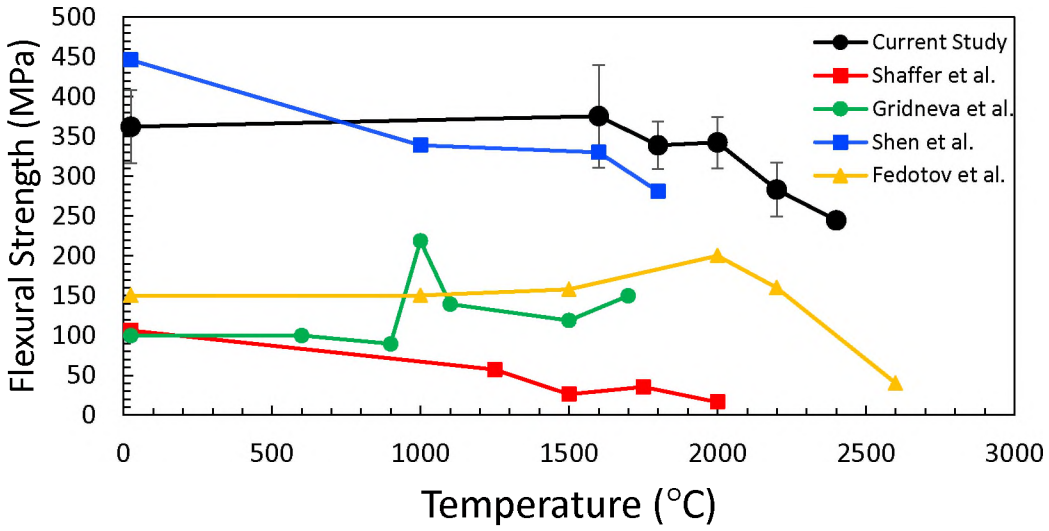

Figure 2. Elevated temperature flexural strength of ZrC_x.

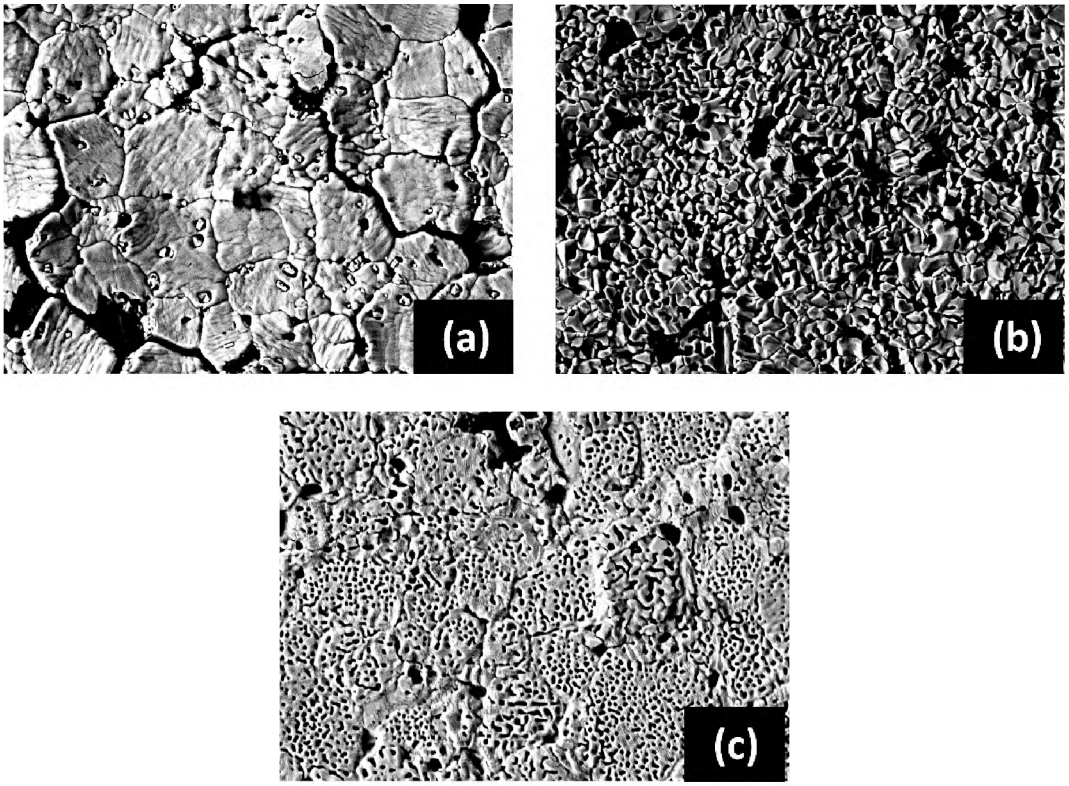

Figure 3. SEM images of the tensile surface of the elevated strength bars at 1800°C (a), 2000°C (b), 2200°C (c).

Table 1. High temperature strength and grain size.

Temperature (°C)	RT	1600	1800	2000	2200	2400
Flexural Strength (MPa)	362 ± 46	375 ± 65	339 ± 30	342 ± 32	283 ± 34	245 ± 14
Tested Bars Grain Size (μm)	2.7 ± 1.4	2.8 ± 1.4	3.1 ± 1.5	3.7 ± 1.5	4.0 ± 1.5	3.7 ± 1.4

REFERENCES

1. X.-G. Wang, J.-X. Liu, Y.-M. Kan, and G.-J. Zhang, "Effect of solid solution formation on densification of hot-pressed ZrC ceramics with MC (M = V, Nb, and Ta) additions," J. Eur. Ceram. Soc., 32 [8] 1795–1802 (2012).

2. G. Vasudevamurthy, T.W. Knight, E. Roberts, and T.M. Adams, "Laboratory production of zirconium carbide compacts for use in inert matrix fuels," J. Nucl. Mater., 374 241–247 (2008).

3. G. Vasudevamurthy, Y. Katoh, J. Aihara, K. Sawa, and L.L. Snead, "Microstructure and mechanical properties of heat-treated and neutron irradiated TRISO-ZrC coatings," J. Nucl. Mater., 464 245–255 (2015).

4. Y. Katoh, G. Vasudevamurthy, T. Nozawa, and L.L. Snead, "Properties of zirconium carbide for nuclear fuel applications," J. Nucl. Mater., 441 [1–3] 718–742 (2013).

5. H.F. Jackson and W.E. Lee, "Properties and Characteristics of ZrC;" pp. 339–372 in Compr. Nucl. Mater. Elsevier Science, London, 2012.

6. M.A. Fedotov and V.P. Yanchur, "Temperture Dependence of the Strength and Placticity of Carbides Obtained by Continuous Saturation," Inorg. Mater., 12 [3] 421–425 (1976).

7. I.V. Gridneva, Y.V. Mil'man, G.A. Rymashevskii, V.I. Trefilov, and S.I. Chugunova, "Effect of temperature on the strength characteristics of zirconium carbide," Powder Metall. Met. Ceram., 15 [8] 638–645 (1976).

8. Y. Shen, X. Wang, and D. Jiang, "Strong ZrC ceramics at high temperatures with the addition of W," J. Am. Ceram. Soc., 102 3090–3096 (2019).

9. A.G. Lanin, P.V. Zubarev, and K.P. Valsov, "Mechanical and Thermophysical Properties of Materials in HTGR Fuel Bundles," At. Energiya, 74 [1] 42–47 (1993).

10. P.T.. Shaffer, D.P.H. Hasselman, and A.Z. Chaberski, "Factors affecting thermal shock resistance of polyphase ceramic bodies," (1962).

11. Harrison RW, Lee WE. Processing and properties of ZrC , ZrN and ZrCN ceramics : a review. Adv Appl Ceram. 2016;115(5):294–307.

SECTION

3. CONCLUSIONS

The research presented in this thesis focused on the properties of ZrC ceramics. More specifically, this research was focused on the baseline properties of near stochiometric ZrC_x. To date many of the studies on ZrC_x do not include important details with respect to the ZrC_x tested. For example, some studies do not include the C/Zr ratio or impurities in the material. Experimentally, the carbothermal reduction method was used to prepare near-stoichiometric ZrC with minimal impurities. Materials were characterized by XRD, SEM, and Raman spectroscopy. The ZrC tested during this study had an average grain size of 2.7 μm ± 1.4 μm with a relative density of ~96%, a secondary graphitic phase was identified using Raman spectroscopy. The strength of ZrC with a C/Zr ratio of 0.92 was 375 ± 65 MPa. The sample had a toughness of 2.9 ± 0.1 $MPa*m^{1/2}$. Vickers hardness was 17 GPa with a load of 1 kgf and 19.5 GPA with a load of 0.5 kgf. The results of the first part of the thesis contributes to the current state of knowledge of ZrC_x mechanical properties. The strength at room temperature correlated with the largest grains in the microstructure. Reducing the size of the largest flaw would be expected to improve the strength of the material.

The mechanical properties of ZrC_x at elevated temperatures were also studied. The strength was measured at elevated temperatures, staying with the standard deviation of room temperature strength until 2200°C where the strength dropped to 283 ± 34 MPa, and then decreased to 245 ± 14 MPa at 2400 °C. The elevated temperature property data is lacking. At elevated temperatures, the mechanical properties can be improved by using

higher purity powders. The higher purity powders and improved processing produced phase pure microstructures with higher densities than seen from the historical studies. The high temperature strength values in older studies tend to be much lower than in the current study, is stable out to 2000°C, showing more promise for extreme environment applications. Controlling the impurities is essential to controlling the mechanical properties of ZrC ceramics. The mechanical properties of the ZrC weaken during exposure to oxidation. ZrC readily oxidizes above 500°C, so finding a way to improve oxidation resistance will be necessary to protect ZrC for structural applications.

4. FUTURE WORK

This research focused on the mechanical properties of ZrC_x at room temperature as well as the high temperature strength of ZrC_x. Several suggestions are presented in this section for advancing understanding and improving the mechanical properties of ZrC_x ceramics.

1. The composition studied in this work was $ZrC_{0.92}$. ZrC_x exists in a wider range of stoichiometries. Further study on the other compositions of ZrC_x will be able to shine a brighter light on the functions of ZrC_x.
2. Varying the grain size of monolithic ZrC_x. It was found in this study that the limiting factor in the strength of at least the room temperature bars was the grain size. Reducing the grain size could increase the strength of ZrC_x. However, finer grain size can enhance the effect of creep and this could prove troublesome at high temperature testing.
3. In addition to different stoichiometries of ZrC_x further study into the oxycarbide formed is needed. Oxygen readily dissolves into the ZrC lattice onto carbon vacancy sites. With ZrC_x ability to retain oxygen finding out the mechanical strengths of oxycarbide with varying oxygen compositions will be able to show how oxygen effects the strengths of ZrC_x in application.
4. Strength was the only mechanical property tested at high temperatures. To more clearly understand the effects of elevated temperatures on ZrC_x other mechanical properties should be tested, fracture toughness, hardness, and elastic modulus.

REFERENCES

1. Wang Y, Liu Q, Liu J, Zhang L, Cheng L. Deposition mechanism for chemical vapor deposition of zirconium carbide coatings. J Am Ceram Soc. 2008;91(4):1249–52.

2. Katoh Y, Vasudevamurthy G, Nozawa T, Snead LL. Properties of zirconium carbide for nuclear fuel applications. J Nucl Mater. 2013;441(1–3):718–42.

3. Gosset D, Dollé M, Simeone D, Baldinozzi G, Thomé L. Structural evolution of zirconium carbide under ion irradiation. J Nucl Mater. 2008;373(1–3):123–9.

4. Vasudevamurthy G, Knight TW, Roberts E, Adams TM. Laboratory production of zirconium carbide compacts for use in inert matrix fuels. J Nucl Mater. 2008;374:241–7.

5. Vasudevamurthy G, Katoh Y, Aihara J, Sawa K, Snead LL. Microstructure and mechanical properties of heat-treated and neutron irradiated TRISO-ZrC coatings. J Nucl Mater. 2015;464:245–55.

6. Fahrenholtz WG, Wuchina EJ, Lee WE, Zhou Y. Ultra-high temperature ceramics: materials for extreme environment applications. Hoboken: John Wiley & Sons; 2014. p. 361–415.

7. Snead LL, Katoh Y, Kondo S. Effects of fast neutron irradiation on zirconium carbide. J Nucl Mater. 2010;399(2–3):200–7.

8. Lonergan JM, McClane DL, Fahrenholtz WG, Hilmas GE. Thermal Properties of Hf-Doped ZrB2 Ceramics. J Am Ceram Soc. 2015;98(9):2689–91.

9. Gosset D. Absorber materials for Generation IV reactors. Structural Materials for Generation IV Nuclear Reactors. Elsevier Ltd; 2017. 533–567 p.

10. Feng L, Fahrenholtz WG, Hilmas GE, Watts J, Zhou Y. Densification, microstructure, and mechanical properties of ZrC–SiC ceramics. J Am Ceram Soc. 2019;(102):5786–95.

11. Wei B, Chen L, Wang Y, Zhang H, Peng S, Ouyang J, et al. Densification, mechanical and thermal properties of ZrC1 − x ceramics fabricated by two-step reactive hot pressing of ZrC and ZrH2 powders. J Eur Ceram Soc. 2018;38(2):411–9.

12. Min-haga E. Sintering and. mechanical properties of ZrC-ZrOa composites. J Mater Sci. 1988;23(1988):2865–70.

13. Sciti D, Guicciardi S, Nygren M. Spark plasma sintering and mechanical behaviour of ZrC-based composites. Scr Mater. 2008;59(6):638–41.

14. Hopkins BJ, Ross KJ. The work function of uranium. Proc Phys Soc. 1962;79(1):447–8.

15. Leipold MH, Nielsen TH. Mechanical Properties of Hot-Pressed Zirconium Carbide Tested to 2600°C. J Am Ceram Soc. 1964;47(9):419–24.

16. Allinson JD, Rivière JC. High temperature, short term, compatibility of some refractory metals with the thermionic converter fuel UC·ZrC. J Nucl Mater. 1965 Oct 1;17(2):97–110.

17. Wang X-G, Liu J-X, Kan Y-M, Zhang G-J. Effect of solid solution formation on densification of hot-pressed ZrC ceramics with MC (M = V, Nb, and Ta) additions. J Eur Ceram Soc. 2012;32(8):1795–802.

18. Jackson HF, Lee WE. Properties and Characteristics of ZrC. In: Comprehensive Nuclear Materials. London: Elsevier Science; 2012. p. 339–72.

19. Harrison RW, Lee WE. Processing and properties of ZrC , ZrN and ZrCN ceramics : a review. Adv Appl Ceram. 2016;115(5):294–307.

20. Pierson HO. 4 - Carbides of Group IV: Titanium, Zirconium, and Hafnium Carbides. In: Pierson HOBT-H of RC and N, editor. Westwood, NJ: William Andrew Publishing; 1996. p. 55–80.

21. Fernandez-Guillermet. Analysis of thermochemical properties and phase stability in the zirconium–carbon system. Am J Alloy Compd. 1995;217(1):69–89.

22. Sara R V. The System Zirconium—Carbon. J Am Ceram Soc. 1965;48(5):243–7.

23. Sarkar SK, Miller AD, Mueller JI. Solubility of oxygen in ZrC. Jounal Am Ceram Soc. 1972;55(12):628–30.

24. David J, Trolliard G, Gendre M, Maître A. TEM study of the reaction mechanisms involved in the carbothermal reduction of zirconia. J Eur Ceram Soc. 2013;33:165–79.

25. Sondhi A, Morandi C, Reidy RF, Scharf TW. Theoretical and experimental investigations on the mechanism of carbothermal reduction of zirconia. Ceram Int. 2013;39(4):4489–97.

26. Maitre A, Lefort P. Solid state reaction of zirconia with carbon. Solid State Ionics. 1997;104:109–22.

27. Gendre M, Maître A, Trolliard G. Synthesis of zirconium oxycarbide (ZrCxOy) powders: Influence of stoichiometry on densification kinetics during spark plasma sintering and on mechanical properties. J Eur Ceram Soc. 2011;31(13):2377–85.

28. Feng L, Lee S, Lee H. Nano-sized zirconium carbide powder: Synthesis and densification using a spark plasma sintering apparatus. Int J Refract Met Hard Mater. 2017;64:98–105.

29. Zhu R, He H, Lin Z, Jiang S, Zhang J. Amorphous/crystalline ZrC alternating multilayers deposited by magnetron sputtering at room temperature. Mater Today Commun. 2020;24(April):101143.

30. Bunshah RF, Nimmagadda R, Dunford W, Movchan BA, Demchishin A V., Chursanov NA. Structure and properties of refractory compounds deposited by electron beam evaporation. Thin Solid Films. 1978;54(1):85–106.

31. Wang X-G, Guo W-M, Kan Y-M, Zhang G-J, Wang P-L. Densification behavior and properties of hot-pressed ZrC ceramics with Zr and graphite additives. J Eur Ceram Soc. 2011;31(6):1103–11.

32. Van Loo FJJ, Wakelkamp W, Bastin GF, Metselaar R. Diffusion of carbon in TiC1−y and ZrC1−y. Solid State Ionics. 1989 Feb 1;32–33:824–32.

33. Silvestroni L, Sciti D. Microstructure and properties of pressureless sintered ZrC-based materials. J Mater Res. 2008;23(7):1882–9.

34. Zhao L, Jia D, Duan X, Yang Z, Zhou Y. Pressureless sintering of ZrC-based ceramics by enhancing powder sinterability. Int J Refract Met Hard Mater. 2011;29(4):516–21.

35. Schönfeld K, Martin HP, Michaelis A. Pressureless sintering of ZrC with variable stoichiometry. J Adv Ceram. 2017;6(2):165–75.

36. Sacks MD, Wang C, Yang Z, Jain A. Carbothermal reduction synthesis of nanocrystalline zirconium carbide and hafnium carbide powders using solution-derived precursors. 2004;9:6057–66.

37. Shen Y, Wang X, Jiang D. Strong ZrC ceramics at high temperatures with the addition of W. J Am Ceram Soc. 2019;102:3090–6.

38. Nachiappan C, Rangaraj L, Divakar C, Jayaram V. Synthesis and densification of monolithic zirconium carbide by reactive hot pressing. J Am Ceram Soc. 2010;93(5):1341–6.

39. Rangaraj L, Chakrabarti T, Kannan R, Jayaram V. Effect of applied pressure on densification of monolithic ZrC x ceramic by reactive hot pressing. J Mater Res. 2016;31(4):506–15.

40. Wei X, Back C, Izhvanov O, Haines CD, Olevsky EA. Zirconium carbide produced by spark plasma sintering and hot pressing: Densification kinetics, grain growth, and thermal properties. Materials (Basel). 2016;9(7).

41. Jackson HF, Jayaseelan DD, Lee WE, Reece MJ, Inam F. Laser Melting of Spark Plasma-Sintered Zirconium Carbide : Thermophysical Properties of a Generation IV Very High-Temperature Reactor Material. Int J Appl Ceram Technol. 2010;7(3):316–26.

42. Wei X, Back C, Izhvanov O, Khasanov OL, Haines CD, Olevsky EA. Spark plasma sintering of commercial zirconium carbide powders: Densification behavior and mechanical properties. Materials (Basel). 2015;8(9):6043–61.

43. Lanin AG, Zubarev PV, Valsov KP. Mechanical and Thermophysical Properties of Materials in HTGR Fuel Bundles. At Energiya. 1993;74(1):42–7.

44. Chang R, Graham LJ. Low-temperature elastic properties of ZrC and TiC. J Appl Phys. 1966;37(10):3778–83.

45. Fedotov MA, Yanchur VP. Temperture Dependence of the Strength and Placticity of Carbides Obtained by Continuous Saturation. Inorg Mater. 1976;12(3):421–5.

46. Gridneva IV, Mil'man YV, Rymashevskii GA, Trefilov VI, Chugunova SI. Effect of temperature on the strength characteristics of zirconium carbide. Powder Metall Met Ceram. 1976;15(8):638–45.

VITA

Nicole Mary Korklan was born in Tucson, Arizona. She is from Tucson, Arizona where she attended high school at Catalina Foothill High School. Nicole graduated high school in the spring of 2012 and moved to Rolla, Missouri to attend Missouri University of Science and Technology later that same year. Nicole received her Bachelor of Science degree in Ceramic Engineering in 2016.

Nicole began her graduate work at Missouri University of Science and Technology in August of 2017. Nicole focused her research on the processing and properties of ZrC ceramics. Nicole received her Master of Science. degree in Ceramic Engineering from Missouri University of Science and Technology in August 2020.